Environmental Science and Pollution Research (2020) 27:39572–39583
https://doi.org/10.1007/s11356-020-09758-1

RESEARCH ARTICLE

# Sulfate removal from mine-impacted water by electrocoagulation: statistical study, factorial design, and kinetics

Caroline Rodrigues[1] · Hioná V. Dal Magro Follmann[1] · Dámaris Núñez-Gómez[1] · Maria Eliza Nagel-Hassemer[1] · Flávio R. Lapolli[1] · María Ángeles Lobo-Recio[1,2]

Received: 25 March 2020 / Accepted: 15 June 2020 / Published online: 10 July 2020


## Abstract

This work aimed to remove sulfate and acidity from mine-impacted water (MIW) via electrocoagulation (EC), a technique which stands as an advanced alternative to chemical coagulation in pollutant removal from wastewaters. The multiple electrochemical reactions occurring in the aluminum anode and the stainless steel cathode surfaces can form unstable flakes of metal hydroxy-sulfate complexes, causing coagulation, flocculation, and floatation; or, adsorption of sulfate on sorbents originated from the electrochemical process can occur, depending on pH value. Batch experiments in the continuous mode of exposition using different current densities (35, 50, and 65 A $m^{-2}$) were tested, and a statistical difference between their sulfate removals was detected. Furthermore, the intermittent mode of exposure was also tested by performing a $2^2$-factorial design to verify the combination with different current densities, concluding that better efficiencies of sulfate removal were obtained in the continuous mode of exposition, even with lower current densities. After 5 h of electrocoagulation, sulfate could be removed from MIW with a mean efficiency of 70.95% (in continuous mode of exposition and 65 A $m^{-2}$ current density), and this sulfate removal follows probable third-order decay kinetics in accordance with the quick drop in sulfate concentration until 3 h of exposure time, remaining virtually constant at longer times.

**Keywords** Acid mine drainage (AMD) · Mine-impacted water (MIW) · Electrocoagulation · Sulfate removal · Decay kinetics · Factorial design

**Abbreviations**

| | |
|---|---|
| AMD | acid mine drainage |
| ANOVA | analysis of variance method |
| EC | electrocoagulation |
| MAV | maximum allowed value |
| MIW | mine-impacted water |
| SD | standard deviation |
| SRB | sulfate-reducing bacteria |

Responsible editor: Ioannis A. Katsoyiannis

**Electronic supplementary material** The online version of this article (https://doi.org/10.1007/s11356-020-09758-1) contains supplementary material, which is available to authorized users.

✉ Caroline Rodrigues
caroline.rodrigues@posgrad.ufsc.br

Hioná V. Dal Magro Follmann
hiona_follmann@hotmail.com

Dámaris Núñez-Gómez
damaris_ng@hotmail.com

Maria Eliza Nagel-Hassemer
maria.eliza@ufsc.br

Flávio R. Lapolli
f.lapolli@ufsc.br

María Ángeles Lobo-Recio
maria.lobo@ufsc.br

[1] Department of Environmental Engineering, Federal University of Santa Catarina (UFSC), Campus Reitor João David Ferreira Lima, Trindade, Florianópolis, SC 88040-900, Brazil

[2] Department of Energy and Sustainability, UFSC, Campus Araranguá, Rod. Gov. Jorge Lacerda,3201, Jardim das Avenidas, Araranguá, SC 88906-072, Brazil

## Introduction

Mining industry is an essential contributor to the world's economy, as it is in Brazil. The process of extraction and beneficiation in coal mining is one of the main economic activities in the Carboniferous basin of southern Santa Catarina State, Brazil (Macan et al. 2012). During the periods of intense drought, in which the hydroelectric power plants cannot work, coal (among other thermoelectric sources) prevents the risk of electrical blackout in Brazil (Brazil 2007). As a part of the Brazilian energy matrix, with over 130 years of mining activity (Silva et al. 2013), the social and environmental impacts of the mines are substantial; almost one thousand abandoned mines exist throughout the Carboniferous basin (Brazil 2018). The active mines are not currently a significant environmental concern because, in theory, the mining companies properly treat their effluents. However, the abandoned and inactive mines produce acid mine drainage (AMD), a heavy metal and rich sulfuric acid effluent, which is a global environmental concern (Demers et al. 2015; Kefeni et al. 2017; Peiravi et al. 2017; Moodley et al. 2018). AMD is produced when sulfidic minerals, like pyrite ($FeS_2$), are exposed to oxygen and water to form sulfuric acid. Therefore, its highly toxic and corrosive characteristics are due to its acidic pH values (between 2 and 4), with high concentrations of sulfate ($SO_4^{2-}$) and dissolved metallic ions (e.g., Fe, Al, Mn, Zn, Cu, and Pb).

The AMD formation constitutes the primary source of pollution of fresh surface waters worldwide (Mesa et al. 2017), known as mine-impacted water (MIW). AMD as well as MIW remediation is a complex process that typically involves acid neutralization and sulfate and dissolved metallic ion removal (Al-Abed et al. 2017). Several physicochemical technologies have been applied to treat this type of effluent, such as reverse osmosis (Masindi et al. 2017); sorption technologies (adsorption and ion exchange) (Silva et al. 2012; Guimarães and Leão 2014); and chemical precipitation as gypsum, barium sulfate, ettringite, jarosite, or ferrite (Tait et al. 2009; Kefeni et al. 2015; Tolonen et al. 2016; Masindi et al. 2017). These technologies can be efficient, and moreover, some have the possibility of metal recovery. However, some disadvantages can be mentioned, like the production of large brine volumes and fouling formation on the membrane due to the gypsum formation (leading to the need of a membrane downstream pretreatment); lowered efficiency of limestone as an adsorbent and precipitant agent in acid conditions; and large volume of sludge and its subsequent treatment, considering that sludges containing barium are of greater concern than those containing sulfate (Silva et al. 2012; Barbosa et al. 2014; Masindi et al. 2017).

Previous studies in our research group (Rodrigues et al. 2019, 2020) have evaluated the biological treatment of MIW biostimulating sulfate-reducing bacteria (SRB), obtaining excellent removals of sulfate (85 and 99.75%) and metallic ions (Fe (≥ 99.04%), Al (≥ 98.47%), and Mn (100%)), and neutralizing pH; however, the sulfide formation increases the toxicity. Additionally, the physical-chemical treatment of MIW and AMD with shrimp shells as a sorption agent has been studied extensively (Núñez-Gómez et al. 2016, 2017a, b, 2018, 2019), and substantial metallic ions (Fe, Al, and Mn) removal and pH neutralization were obtained, although the sulfate anion remained as a challenge in the treatment of these effluents. Due its high solubility and stability in aqueous solutions, sulfate is not easily removed from water (Mamelkina et al. 2017). The adverse effects include (i) increased dissolved solids of the receiving waterbody, affecting its usefulness downstream for drinking, irrigation, or industry (Moosa et al. 2005); (ii) can cause problems of odor and corrosion to concrete buildings (Mamelkina et al. 2017); and (iii) the ingestion of water containing above 500 mg $L^{-1}$ can cause diarrhea (Najib et al. 2017).

Therefore, a new technology for sulfate removal was tested: electrocoagulation (EC). Several recent studies (Mamelkina et al. 2017, 2019; Nariyan et al. 2017, 2018) have addressed this type of treatment in MIW. The EC treating MIW stands as a promising technology, providing better efficiencies for sulfate removal at low pH (characteristic of MIW) than at higher pH values, because in acidic conditions, the numerous cationic species can interact electrostatically with the anions (Mamelkina et al. 2017), forming precipitates, while at neutral and alkaline pH, the mechanism is different: the primary coagulant species are amorphous metal hydroxide precipitates that according to the surface charge can adsorb ions in its surface (Mamelkina et al. 2017). Additionally, these precipitates can be positively or negatively charged (because of the adsorption of hydroxometallic ions on the surface), with a large number of possibilities for the fixation of sulfate ions (Mamelkina et al. 2017). The sulfate ions are attracted to the charged precipitates and form metallic hydroxysulfates with high adsorption properties. These hydroxysulfates form larger structures and sweep through the water (coagulation) (Singh and Ramesh 2014). Furthermore, the process can generate a more neutral pH (range of 6–7) and compact sludge, when compared with conventional coagulation (Nariyan et al. 2017). In the EC process, considered to be efficient and environment-friendly method (Wu et al. 2019), various anodes can be used, but Al and Fe are superior metals for producing multivalent ions, favoring the processes. Not coincidentally, these are the most common anodes used as electrodes in EC (An et al. 2017; Nariyan et al. 2017); generally, the Al electrode in acidic medium (pH < 6) is used, and in neutral and alkaline medium, the Fe electrode is more suitable (Bener et al. 2019).

In the EC technology (summarized in Fig. 1), oxidation and reduction occur simultaneously. On the anode surface (framed in red), the oxidation reaction occurs, causing the dissolution

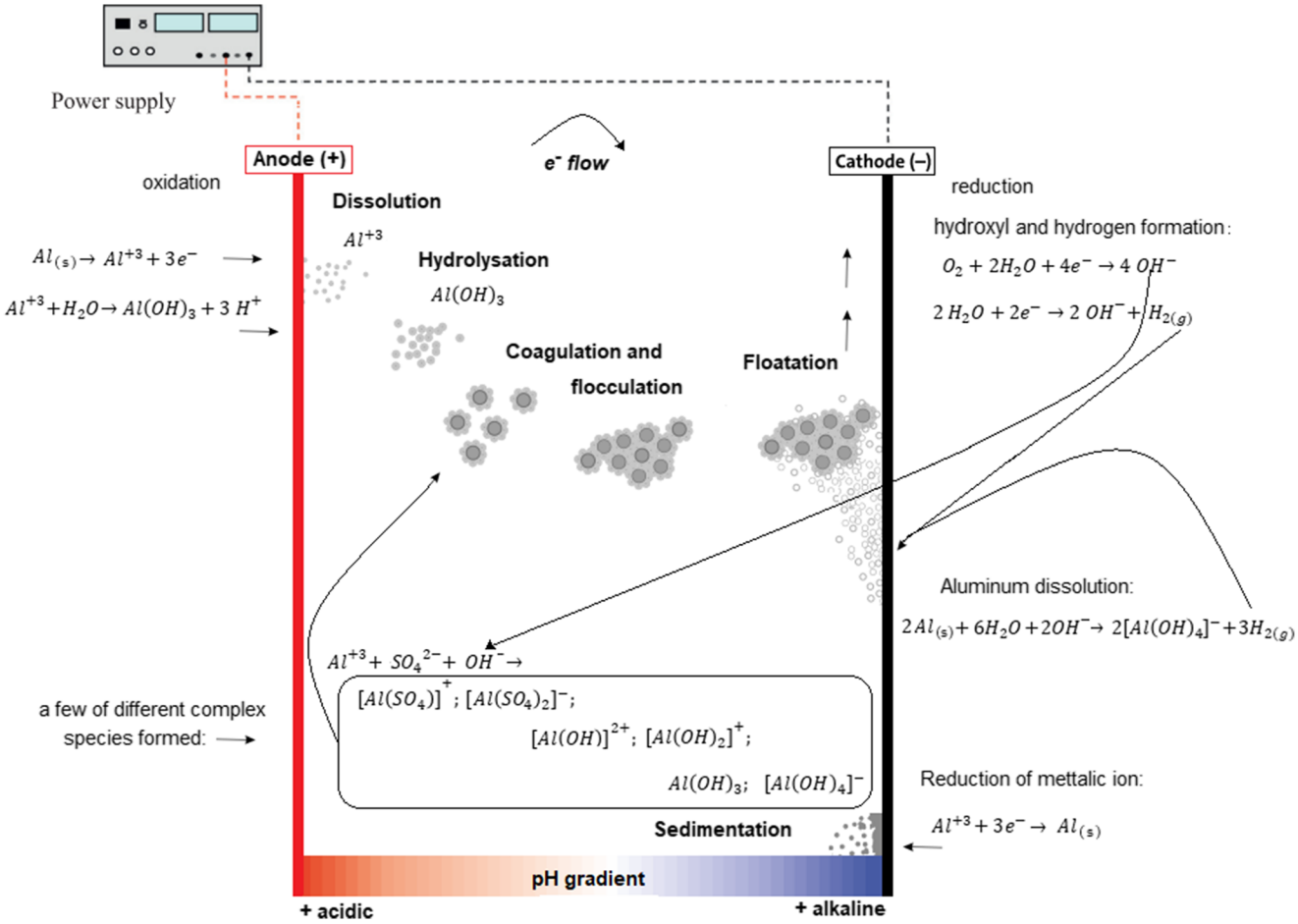


**Fig. 1** EC scheme: the numerous unstable species formed start to aggregate, initiating the coagulation, flocculation, and floatation. Adapted from (Sánchez-España 2007; Vepsäläinen 2012; Nariyan et al. 2017)

and hydrolysis of the $Al^0$, releasing $Al^{3+}$ into the medium, which binds with the hydroxide ions ($OH^-$) produced from the cathode surface reduction (framed in black), as well as with the sulfates in solution, thus giving rise to aluminum sulfate complexes that form colloidal particles (Vepsäläinen and Sillanpää 2020). Colloids are stable in water due to the net interactions between electrostatic repulsions and attractive van der Waals interactions between the particles (Shamaei et al. 2018; Vepsäläinen and Sillanpää 2020). In the coagulation process, these colloidal particles are destabilized because the repulsive energy between them is reduced by the presence of a coagulant, being more easily agglomerated. Flocculation occurs when these agglomerated particles attach to each other with the formation of a weak bond (van der Waals forces) with force inversely proportional to the distance from particle surface, as described by the DLVO (Derjaguin, Landau, Verwey, and Overbeek) theory (Adair et al. 2001; Shamaei et al. 2018). Once formed, these flocs will be floated (adhered to bubbles) by the hydrogen produced at the cathode (Vepsäläinen et al. 2011, 2012). Furthermore, the removal also may occur as sedimentation (for higher density particles). At pH ≥ 5.5, formation of insoluble aluminum hydroxides occurs (Sánchez-España 2007), and sulfate removal can also be effected via an adsorption process (Nippatla and Philip 2019; Follmann et al. 2020).The rate of electrochemical reactions is proportional to the current density (Shamaei et al. 2018), and at alkaline pH, it can be lower than the value calculated by Faraday's law, indicating that other reactions at the anode may be occurring (Vepsäläinen 2012).

When handling a series of experiments, statistical methods can be used in order to establish its dependence on the variables involved in the process. Therefore, the factorial design stands as a technique that allows the combination of all variables at all levels, obtaining the simultaneous effect of each variable over the response. The $2^k$ factorial design is the simplest type of factorial design, which involves two or more independent variables (named factors (k)) in two levels (+1 and −1), being very useful during the initial stages of the study when there are many variables to investigate, providing the lowest number of runs in a complete factorial design (Calado and Montgomery 2003).

In this sense, this work aimed to evaluate the EC processes for the MIW sulfate removal, under different current densities (35, 50, and 65 A $m^{-2}$). As EC involves electric energy,

different modes of exposure (continuous and intermittent) were tested. The relation between the independent variables (exposure mode and current density) was evaluated by means of a $2^2$-factorial design. Moreover, a kinetics study for the assay with the highest removal of sulfate was performed.

## Material and methods

### MIW collection and analytical methods

MIW from the Sangão River (inside the Carboniferous basin of southern Santa Catarina State, Brazil) was used for the treatment tests. The samples were collected, filtered under vacuum through a 0.45-μm pore membrane, as described in the references (Núñez-Gómez et al. 2016, 2017a; APHA 2017; Rodrigues et al. 2019, 2020), and characterized. The sulfate concentration was determined before and after the EC tests, by photocolorimetry on a HACH 5000 Spectrophotometer using colorimetric kits Sulfaver HACH, compatible with the *Standard Methods for the Examination of Water and Wastewater* procedure (APHA 2017). Likewise, for the metallic ions (Fe, Al, and Mn) initial characterization, the HACH colorimetric kits were also used (ferrover, aluminon, and periodate oxidation, respectively). These metals were selected since they are the most commonly found in AMD from abandoned coal mines (Seo et al. 2017). The total organic carbon was measured as non-purgeable organic carbon (NPOC) in the high-temperature combustion method (APHA 2017) (Shimadzu TOC-LCSH), and the pH was monitored with a Thermo Fisher Scientific pHmeter.

### Experimental setup for electrocoagulation

An electrochemical system was mounted for bench-scale testing, adapted from Mamelkina et al. (2017). The system consisted of replicates of the EC reactors in parallel to execute experiments in duplicate and triplicate. Each EC reactor consisted of a 1-L plastic beaker, in which flat plate electrodes of Al (anode) and stainless steel (cathode) were immersed, spaced 5 cm from each other. The electrodes had the dimensions of 5.65 × 13.9 cm, with a useful area of 28.76 $cm^2$ (anode). A magnetic stirrer was used to homogenize the samples because a chemical species concentration gradient naturally occurs. The passage of electric current from the power supply (PS-A305D) to the reactors was regulated by a control panel, providing continuous or intermittent current exposure that went into the reactors with the same electric current intensity (Fig. 2).

Three experiments were carried out in triplicate with three different current intensities under the continuous mode of exposure: 0.101, 0.144, and 0.187 A, yielding current densities of 35, 50, and 65 A $m^{-2}$, respectively. For all experiments, 1 L of MIW per beaker was used, the temperature was controlled at 23 ± 1 °C, and the total time of electric current passage was 5 h under agitation. Samples were taken hourly and filtered under vacuum (0.45-μm pore membrane filter), and the pH and sulfate concentration were then measured. The data obtained was then used for statistical study and to determine the appropriate kinetics.

### Statistical study

Sulfate removal data for current densities 35, 50, and 65 A $m^{-2}$ and EC times of 3, 4, and 5 h were evaluated by the analysis of variance method (ANOVA), and the difference between the means was evaluated using the Tukey test, at a 95% confidence level ($p \leq 0.05$). These analyses were performed using the R software (v3.6.3, 2020).

### Kinetics studies

The order ($n$) of a reaction is defined as the exponent of the species concentration in the rate equation and generally is expressed in empirical quantities, deduced from observed behavior (Helfferich 2004). The rate equation is expressed in Eq. (1) and is valid for irreversible reactions in a homogenous reactor (Fogler 1999). When the mechanism is not known, a trial-and-error solution is often attempted to fit the data with empirical rate equations of $n^{th}$ order obtained from the integral method (Levenspiel 1999). In the integral method of analysis, the rate equation after appropriate integration and mathematical manipulation generates Eq. (2), where $C$ is the sulfate concentration at time $t$, $C_0$ is the initial concentration, $n$ is the kinetics order, and $k_n$ is the $n^{th}$-order reaction constant.

$$-\frac{dC}{dt} = k_n C^n \tag{1}$$

$$\frac{1}{C^{n-1}} = \frac{1}{{C_0}^{n-1}} + (n-1)k_n t, \quad for\ n \neq 1 \tag{2}$$

If a reasonably linearity is obtained, then the rate equation is said to satisfactorily fit the data. Generally, it is suggested that integral analysis is attempted first (due its higher accuracy), and, if not successful, the differential method is then tried. Although the latter requires larger amounts of data, the differential method is a useful tool in uncertain situations (Levenspiel 1999). The differential method of analysis deals directly with the differential rate equation to be tested (Eq. (3)), evaluating all the terms in the derivative equation and examining the quality of the experiment equation fit.

$$log\left(-\frac{dC}{dt}\right) = log k_n + n\ log C \tag{3}$$

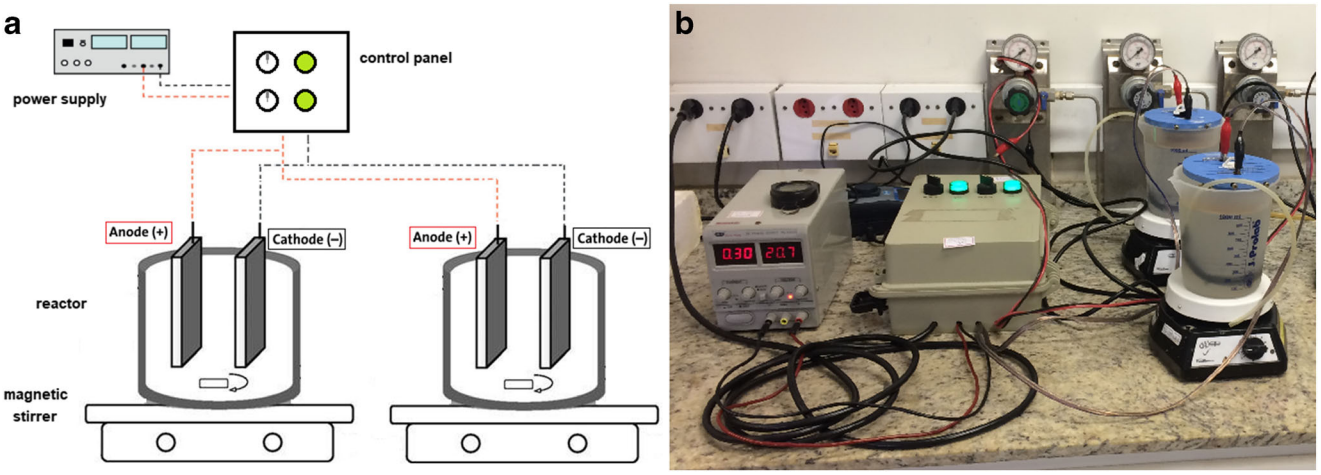


**Fig. 2** ***a*** An illustration and ***b*** a photograph of the EC tests, operated in laboratory scale.

## Factorial design

The influence of the different current densities with different exposure modes on the sulfate removal from MIW was investigated, using the $2^2$-factorial design in duplicate with the central point in triplicate. The factor scores (−1 and + 1) indicate the minimum and maximum level for each test of the variables, and the central point (0) is the symmetrical distance between both, as shown in Table 1.

The mode of exposure and current density were the independent variables (*k*), and as the dependent variable (response), the efficiency of sulfate removal (%) after 5-h treatment was selected. Therefore, the combination of all variables provided seven experiments, which were determined by the Statistica software, following the matrix in Table 1. The sulfate removal was evaluated by the analysis of variance ANOVA, Pareto diagrams, and response surface (3D and 2D) graphs, using the Statistica 8 software (Statsoft, Inc.).

## Results and discussion

### pH rise and sulfate removal in continuous mode of exposure

Initially, the MIW pH was 3.30 and the sulfate concentration was 210 mg $L^{-1}$ (for the 65 A $m^{-2}$ assay) and 190 mg $L^{-1}$ (for the 35 and 50 A $m^{-2}$ assays). This difference on the sulfate concentration values is because the assays were performed in different days, and it is known that MIW composition varies over time. The metallic ions concentrations were 29.4, 11.24, and 2.0 mg $L^{-1}$, for Fe, Al, and Mn, respectively, and the non-

**Table 1** Factorial design results for sulfate removal efficiency by EC

| Independent variable/ (level) | | (−1) | 0 | (+1) |
|---|---|---|---|---|
| Current density (A $m^{-2}$) | | 35 | 50 | 65 |
| Mode of exposure (on/off)[a] | | 5/0 (continuous) | 5/5 | 5/10 |
| | Independent variables | | Dependent variable | |
| | Current density | Mode of exposure | Efficiency (% removal) | Mean efficiency ± SD[b] |
| Experiment 1 | 35 | 5/0 | 63.68<br>66.84 | 65.26 ± 2.23 |
| Experiment 2 | 65 | 5/0 | 72.38<br>69.52 | 70.95 ± 2.02 |
| Experiment 3 | 35 | 5/10 | 18.33<br>10.00 | 14.17 ± 5.89 |
| Experiment 4 | 65 | 5/10 | 44.71<br>45.88 | 45.29 ± 0.83 |
| Experiment 5 | 50 | 5/5 | 51.11 | 50.37 ± 2.31 |
| Experiment 6 | 50 | 5/5 | 52.22 | |
| Experiment 7 | 50 | 5/5 | 47.78 | |

[a] (minutes on/minutes off) of electric current

[b] *SD* standard deviation

purgeable organic carbon was 0 mg $L^{-1}$. Although the sulfate concentrations in these samples did not exceed the maximum allowed value (MAV) by the Brazilian normative (250 mg $L^{-1}$ for freshwater) (Brazil 2011), sulfate removal is important due to sulfate-reducing bacteria, capable of transforming sulfate into toxic sulfide, in the Sangão River (Rodrigues et al. 2020), where the MAV cannot exceed 0.3 mg $L^{-1}$ in Class III freshwater (adequate for reuse as non-potable) (Brazil 2005). Figure 3a shows the pH variations over electric current flow and time. The 50- and 65-A $m^{-2}$ current density curves presented a similarly high slope with the corresponding increase in pH until 3 h, and, after that, a smoother curve was produced. In contrast, with the 35-A $m^{-2}$ curve, the pH rise was less pronounced.

Although, for the 3 current densities tested, at the end of the 5-h experiment, the final pH values were not under 7.70 (7.70 ± 0.27, 8.75 ± 0.14, and 8.06 ± 0.42 for 35, 50, and 65 A $m^{-2}$, respectively). The pH rise is probably derived from the hydrolysis reactions that occur at the cathode, generating hydroxyl anions ($OH^-$). The rate of the electrochemical reaction is directly proportional to the current density, and the test with the lowest current density (35 A $m^{-2}$) corroborates this: less hydroxyl was produced, so its pH was slightly lower, though very close to the other two currents tested. Analogously, in the sulfate decay curves (Fig. 3b), at the lowest current density, less sulfate was removed (i.e., a lower rate of sulfate decay had occurred) when compared with other current densities. For the sulfate concentration, the 65- and 50-A $m^{-2}$ curves followed the same pattern of decay: until 2 h presented a higher decay and, after that, a smoother curve came out, with very similar sulfate concentrations over time. For the 65 A $m^{-2}$, the sulfate concentration decay was faster after 1 h. The 35-A $m^{-2}$ assay presented a much smoother decay in the first 2 h. However, at the end of 5 h, the concentrations of the three assays were similar (≤ 65.33 mg $L^{-1}$).

In relation to sulfate concentration over time, ANOVA showed no significant difference between 3, 4, and 5 h for the current density of 65 A $m^{-2}$ ($p$ = 0.3930). In contrast, for the 50-A $m^{-2}$ current density, the ANOVA showed difference between them ($p$ = 0.0294): the Tukey test showed no difference between 4 and 5 h ($p$ = 0.9840) but presented difference between 3 and 5 h ($p$ = 0.0396) and between 3 and 4 h ($p$ = 0.0486). Consequently, viewing the lowest power consumption, 50-A $m^{-2}$ current density during 4-h EC, or 65 A $m^{-2}$ with 3-h EC time, can be chosen as convenient treatment conditions. Furthermore, an estimation based on Faraday's law indicates that both conditions are release to the medium approximately the same Al mass (67.11 g and 65.44 g for 50 A $m^{-2}$ during 4 h and 65 A $m^{-2}$ during 3 h, respectively) and then, a similar power consumption can be deduced (see supplementary material, Eq. S1 and Fig. S1).

According to the speciation diagram of aluminum in AMD (Sánchez-España 2007), several aluminum sulfate complexes are formed at pH 0–6.5, $Al(OH)_3$ precipitates at pH 5.5–8, and the formation of soluble aluminate occurs at pH ≥ 6. Thus, the sulfate removal via flocculation/coagulation until 2 h of exposure time (formation of $AlSO_4^+$ and $Al(SO_4)_2^-$) and participation of adsorption on $Al(OH)_3$ between 2 and 3 h can be suggested. After 3 h of exposure time, in the 50- and 65-A $m^{-2}$ cases, pH is near of 8 and then aluminum from anode remains mostly dissolved as aluminate and sulfate removal does not occur (Fig. 3). Consequently, it can be deduced that pH values > 8 are not adequate for removing sulfate via electrocoagulation processes.

The mean efficiency obtained for sulfate removal in each test after 5 h (Fig. 4A) indicates that values were also close in terms of removal. The mean efficiencies obtained were 65.26 ± 2.23, 69.12 ± 2.65, and 70.95 ± 2.02 (% sulfate removal) for the current densities 35, 50, and 65 A $m^{-2}$, respectively. However, the ANOVA showed that there was a significant difference in the removal efficiencies ($p$ = 0.0432). To compare the difference between the means of each treatment, the Tukey test was performed. The 65-A $m^{-2}$ assay differs statistically from the 35 A $m^{-2}$ ($p$ = 0.0387), but the 50-A $m^{-2}$ assay does not differ statistically from either the 35 A $m^{-2}$ ($p$ = 0.1582) or the 65 A $m^{-2}$ ($p$ = 0.5364). This comparison is also illustrated in the alignment of the error bars in Fig. 4a: the bar corresponding to the assay at 50 A $m^{-2}$ (orange) is aligned with the others' efficiency bars, but the 65-A $m^{-2}$ (gray) bar is not aligned with the 35-A $m^{-2}$ bar (blue). Figure 4b shows the

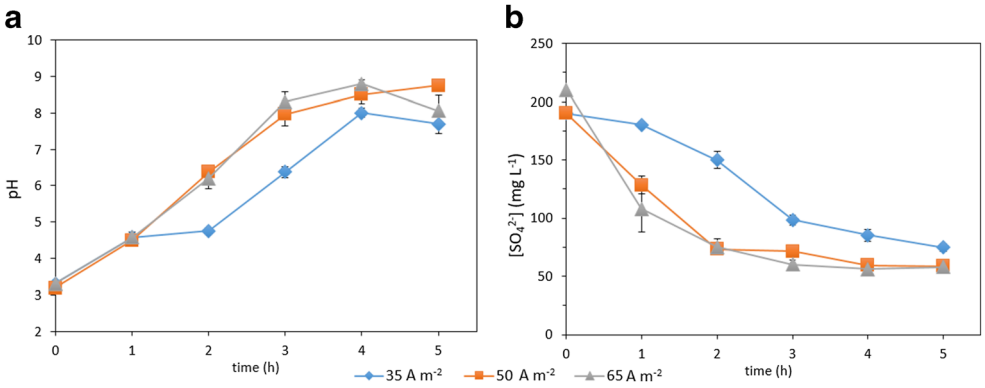


**Fig. 3** **a** pH and **b** sulfate concentration decay profile for the different electric current densities tested. The data points represent triplicate average values and the error bars represent the standard deviation

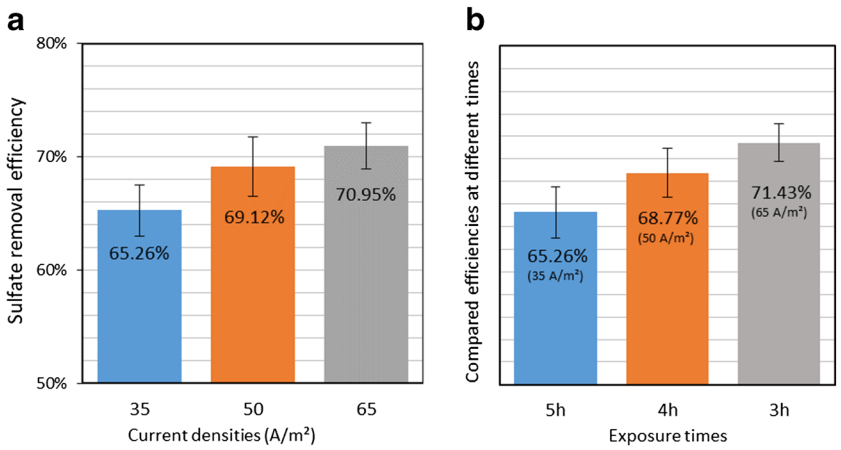


**Fig. 4** **a** Efficiencies for sulfate removal after 5 h of continuous mode of exposure. **b** Comparison of the best sulfate removal efficiency for each current density (at different times of exposure). The bars represent the standard deviation of the mean values

best sulfate removal efficiency for each current density (at different times), reiterating that the 65 A $m^{-2}$ with 3-h time can be chosen as convenient treatment conditions, as stated before in the ANOVA analysis.

A small number of studies regarding the removal of sulfate via EC were found, in which substantially different experimental conditions were used: Hossini et al. (2015) reached approximately 85% sulfate removal from a synthetic wastewater at pH 8 with 80 mg $L^{-1}$ sulfate using an iron anode and a current density of 120 A $m^{-2}$ for 90-min EC time. Nariyan et al. (2017) reached a 41% removal from real AMD containing 13,000-mg $L^{-1}$ sulfate after 2-h EC time using 700-A $m^{-2}$ current density. Higher EC times had not been tested. In the current research, 64.29% sulfate removal was reached after 2-h treatment (65 A $m^{-2}$ assay), although it progressed to 71.43% after 3 h and oscillated to 70.95% after 5 h (Fig. 4). The comparison of these results seems to confirm that very high current densities do not improve the sulfate removal when aluminum anode is used, because the high pH elevation drives to the formation of soluble aluminate (Kaur et al. 2018), which does not contribute to the EC process. Tait et al. (2009) studied precipitation in the form of gypsum crystallization for sulfate-contaminated wastewaters with high concentrations (up to 11,400 mg $L^{-1}$), concluding that the method is effective for considerably high concentrations but limited for low sulfate concentrations. Therefore, it can be inferred that EC is potentially an adequate method for relatively low sulfate concentrations and precipitation is effective for higher concentrations.

## Kinetics study over the highest sulfate removal assay

A kinetics study of the sulfate removal was performed because a decay on the sulfate concentration over time was evident. The determination of the kinetic reaction order was carried out for the 65-A $m^{-2}$ continuous mode of exposure assay because this condition showed the best sulfate removal after 5 h. Several $n$ values were considered (ranging from 0 to 4, in 0.5 increments), and $k_n$ was calculated according to the corresponding equations (Eq. (2)). In Table 2, the calculations are listed in descending order of the coefficient of determination ($R^2$) from the tested kinetic equations.

As Table 2 indicates, three different orders reached high and similar $R^2$ ($n$ = 3, 3.5, and 2.5, providing $R^2$ = 0.9857, 0.9820, and 0.9809, respectively). Therefore, as a complementarily test and as tiebreaker criteria, the differential method was tested (Eq. 3), and Fig. 5 shows the corresponding plot.

Through linear regression, the angular coefficient gives $n$ that approaches 3 (2.9036). Therefore, it indicates that the kinetic is of third order. The $k_3$ value obtained from the differential method was $2.8 \times 10^{-5}$ $L^2$ $mg^{-2}$ $h^{-1}$, relatively close to the $k_3$ value from the integral method ($4 \times 10^{-5}$ $L^2$ $mg^{-2}$ $h^{-1}$, Table 2). A sulfate decay kinetics of third order implies in a high and a low decay rate at high and low sulfate concentrations, respectively. This is in agreement with the behavior observed in the Figure 3b, in which the sulfate concentration drops quickly until 3 h of exposure time remaining virtually constant between 3 and 5 h. The kinetic studies of sulfate decay are controversial, and there is no general agreement between the various authors. Hossini et al. (2015) proposed first-order kinetics, and Nariyan et al. (2017) proposed a second-order model on the basis of the $R^2$ value only, and other orders have not been tested.

Considering that each point of the data had been obtained from triplicate experiments, the temperature was controlled and constant (23 ± 1 °C), and both methods (differential and integral) converged to similar values of $k_3$; there is sufficient rationale to consider $n$ = 3 to be adequate. As the integral method has higher accuracy, the $k_3$ generated by this method was considered.

## Factorial design

A factorial design was carried out to verify the best combination between the values of the independent variables (factors) selected: current density and mode of exposure,

**Table 2** Sulfate decay kinetics tested obtained from the integral method for 65 A·m$^{-2}$.

| $R^2$ | Order ($n$) | Linearized Equation | Linear regression | $k_n$ | $k_n$unit |
|---|---|---|---|---|---|
| 0.9857 | 3 | $\frac{1}{C^2} = \frac{1}{C} + 2kt$ | $\frac{1}{C^2} = 2 \times 10{-}5 + 8 \times 10{-}5t$ | $4{\times}10^{-5}$ | $L^2{\cdot}mg^{-2}\ h^{-1}$ |
| 0.9820 | 3.5 | $\frac{1}{C^{2.5}} = \frac{C_0\,1}{C_0^{2.5}} + 2.5kt$ | $\frac{1}{C^{2.5}} = 2 \times 10{-}7 + 1 \times 10{-}5t$ | $4{\times}10^{-6}$ | $L^{2.5}{\cdot}mg^{-2.5}\ h^{-1}$ |
| 0.9809 | 2.5 | $\frac{1}{C^{1.5}} = \frac{1}{C_0^{1.5}} + 1.5kt$ | $\frac{1}{C^{1.5}} = 4 \times 10{-}4 + 5 \times 10{-}4t$ | $3.3{\times}10^{-4}$ | $L^{1.5}{\cdot}mg^{-1.5}\ h^{-1}$ |
| 0.9731 | 4 | $\frac{1}{C^3} = \frac{1}{C_0^3} + 3kt$ | $\frac{1}{C^3} = 3 \times 10{-}7 + 2 \times 10{-}6t$ | $6.7{\times}10^{-7}$ | $L^3{\cdot}mg^{-3}\ h^{-1}$ |
| 0.9643 | 2 | $\frac{1}{C} = \frac{1}{C_0} + kt$ | $\frac{1}{C} = 5.7 \times 10{-}3 + 3.4 \times 10{-}3t$ | $3.4{\times}10^{-3}$ | $L{\cdot}mg^{-1}\ h^{-1}$ |
| 0.9338 | 1.5 | $\frac{1}{\sqrt{C}} = \frac{1}{\sqrt{C_0}} + 0.5kt$ | $\frac{1}{\sqrt{C}} = 0.0763 + 0.0162t$ | 0.0324 | $L^{0.5}{\cdot}mg^{-0.5}\ h^{-1}$ |
| 0.8896 | 1 | $\ln C = \ln C_0 - kt$ | $\ln C = 5.1395 - 0.3231t$ | 0.3231 | $h^{-1}$ |
| 0.8354 | 0.5 | $\sqrt{C} = \sqrt{C_0}{-}0.5kt$ | $\sqrt{C} = 13.087{-}1.6662t$ | 3.3324 | $mg^{0.5}{\cdot}L^{-0.5}\ h^{-1}$ |
| 0.7771 | 0 | $C = C_0 - kt$ | $C = 173 - 35.6t$ | 35.6 | $mg{\cdot}L^{-1}\ h^{-1}$ |

as well as their influence level in the treatment. The current density was selected because a statistically significant difference in the sulfate removal efficiency was found as a function of the current density value. The mode of exposure was also varied (continuous and intermittent) to find the best condition with the lowest possible power consumption.

Therefore, seven tests were performed according to the $2^2$-factorial design, in duplicate with center point in triplicate, with exposure time of 5 h for each. Table 1 contains the matrix with all combinations of the independent variables tested, as well as the corresponding dependent variables (responses), and the mean and standard deviations of the tests were performed in duplicate and triplicate. The ANOVA showed that the model presented for sulfate removal was significant ($F_{\text{calculated}} > F_{\text{Tabulated}}$, for all factors that substantially affected the sulfate removal) (Table 3). Complementarily, the model was validated by the distribution of residuals (Fig. 6a). The predicted values by the model (red line) and the observed values (blue circles) are significantly similar, showing a strong correlation between them with an excellent adjustment

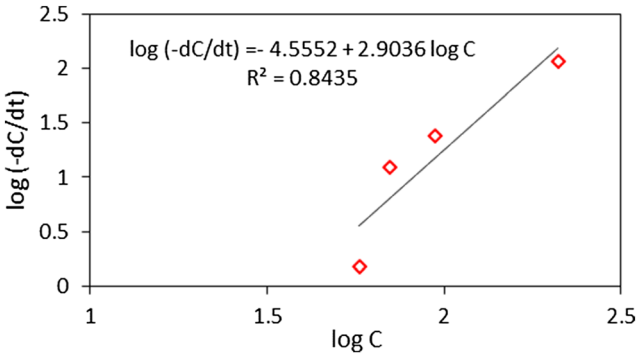


**Fig. 5** Graphical determination of the sulfate decay reaction order by the differential method: the curve slope is the order ($n$), and the intercept is the logarithm of $k_n$.

(99.28%) of the mathematical model, indicating that this model is predictive for sulfate removal.

When performing the factorial design, the influence of each variable over the response, as well as the interaction between them, must be identified. From the Pareto chart (Fig. 6b), the effect of each variable tested can be identified, with the interaction between them for sulfate removal, at a confidence level of 95% ($p \leq 0.05$). The current density variable positively influenced the sulfate removal: the higher current density applied the greater removal is obtained. For the mode of exposure variable, the influence was negative: so, the longer the current was off, the amount of sulfate removed decreased. Nevertheless, the interaction between these two variables is positive: when a higher current density (positive) with more time off (negative) is combined, the removal capacity is increased. These results confirm that lower current densities or shorter exposure times release a lower amount of $Al^{3+}$ to the medium, i.e., a lower amount of coagulant and, consequently, a lower sulfate removal are attained.

Considering that the variance analysis showed that sulfate removal was significantly affected by both factors individually as well as the interaction between them ($p < 0.05$, Table 3), the variables' influence was analyzed on response surface plots to determine the level for each factor that provides the highest removal efficiency for the parameter. Figure 6c shows the 3D contour curve graph, and Fig. 6d shows the 2D response surface for sulfate removal. Analyzing the mode of exposure, the continuous (5/0) provided better sulfate removal, with efficiencies > 70% for current densities between 50 and 65 A m$^{-2}$, in agreement with Fig. 4. If the exposure is intermittent (5/5 and 5/10), lower efficiencies occur for all current densities tested, as above deduced from the Pareto chart. The best sulfate removal (70.95 ± 2.02%) was obtained with continuous mode of exposure and a current density of 65 A m$^{-2}$.

**Table 3** Analysis of variance for the sulfate removal variables in $2^2$-factorial design

| Factor | SS | df | MS | $F_{Calc}$ | $F_{Tab}$[a] | $p$ |
|---|---|---|---|---|---|---|
| Current density (CD) | 338.744 | 1 | 338.744 | 71.0904 | 9.28 | 0.003501 |
| Exposure mode (EM) | 1472.641 | 1 | 1472.641 | 309.0553 | 9.28 | 0.000401 |
| CD by EM | 161.671 | 1 | 161.671 | 33.9291 | 9.28 | 0.010077 |
| Error | 14.295 | 3 | 4.765 | | | |
| Total SS | 1987.351 | 6 | | | | |

*SS* sum of squares, *df* degrees of freedom, *MS* mean square, *F* factor F, *p* probability

[a] Tabulated values for a 95% confidence level (Box et al. 1978)

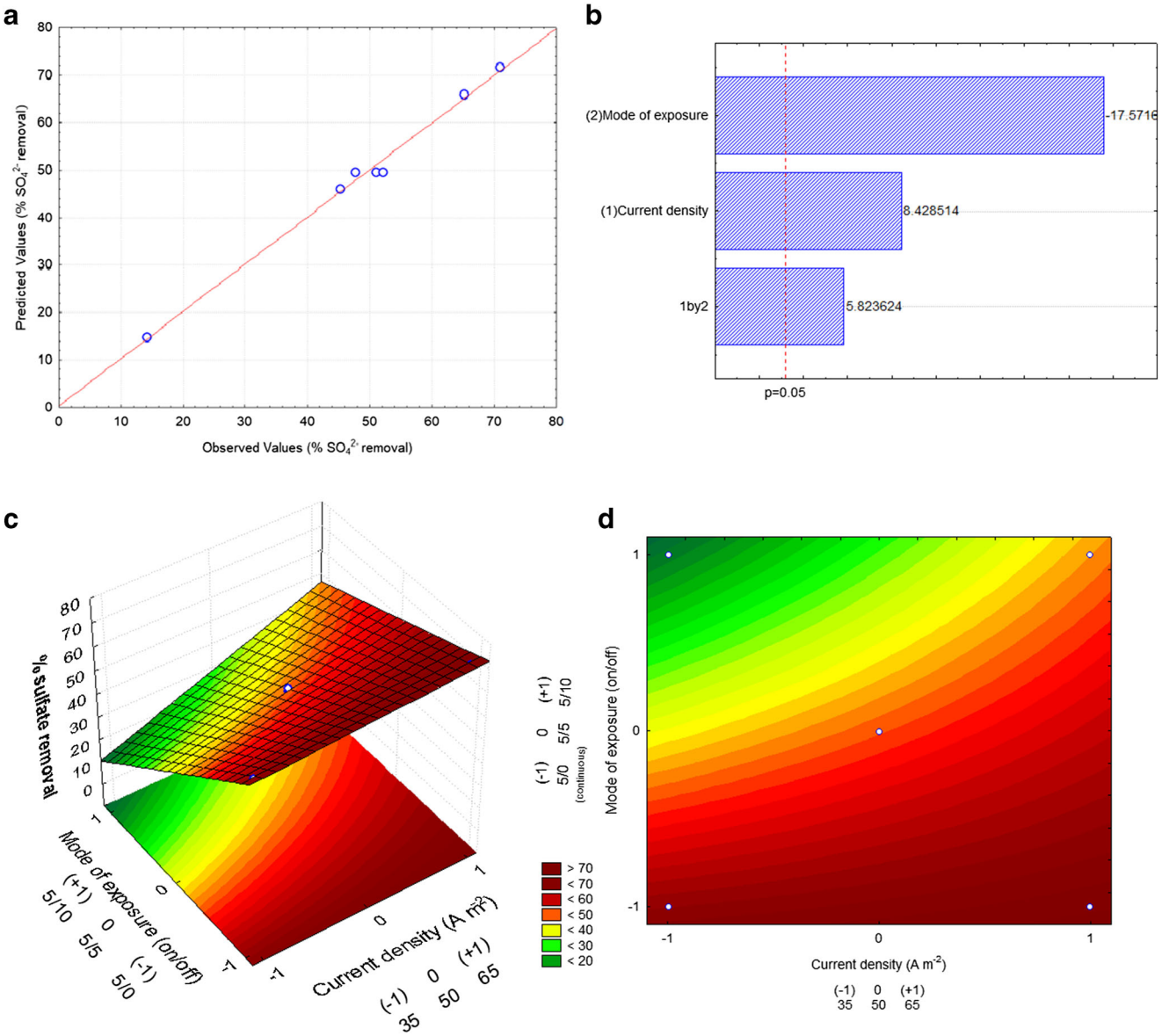


**Fig. 6** ***a*** Residual distribution for the sulfate removal, indicating the goodness of fit ($R^2 = 0.9928$) and ***b*** Pareto chart over the variables and the interaction between them. ***c*** Contour curve and ***d*** response surface for % sulfate removal

## Conclusions

This study has demonstrated that EC is a valuable sulfate removal alternative when compared with conventional precipitation methods, especially for relatively low sulfate concentrations. A minimum current density of 50 A $m^{-2}$ along with 4 h of continuous mode of exposure, or a 65-A $m^{-2}$ assay along with 3 h, is convenient for an effective performance.

The sulfate removal from MIW by EC on the assays with continuous modes of exposure to the electric current yielded plausible efficiencies of up to 70.95 ± 2.02% (65 A $m^{-2}$). With these conditions, the results were better than other studies with significantly higher current densities, although the relatively low removal percentages show the difficulty in the sulfate removal from MIW. The kinetics study showed that this sulfate removal follows a third-order decay. EC was also efficient in increasing the pH values in the MIW to values between 7.70 and 8.75. The incomplete removal of sulfate is tentatively attributed to too high pH values (pH > 8) and/or the third-order kinetic decay.

The factorial design showed that the continuous mode of exposure, together with 65-A $m^{-2}$ current density, is the best condition for sulfate removal from MIW by EC, proving that an intermittent mode of exposure does not achieve the same effect. The mathematical model of linear regression obtained from the response surface methodology presented an excellent adjustment to the original model.

As a continuation of this research, the effects of initial pH, initial sulfate concentration, and metallic ions (Fe, Al, and Mn) removal on EC are being thoroughly studied.

**Author contributions** Caroline Rodrigues has contributed for the conceptualization, methodology, investigation, writing the original draft, and review and editing the manuscript; Hioná V. Dal Magro Follmann for the software, investigation, and formal analysis; Dámaris Núñez-Gómez for the conceptualization, methodology, and writing the original draft; Maria Eliza Nagel-Hassemer for writing, reviewing, and editing; Flávio R. Lapolli for project administration and funding acquisition; and María Ángeles Lobo-Recio for the conceptualization, supervision, writing, reviewing, and editing.

## Compliance with ethical standards

**Conflict of interest** The authors declare that they have no conflict of interest.

## References


Adair JH, Suvaci E, Sindel J (2001) Surface and colloid chemistry. Encycl. Mater. Sci. Technol. 1–10

Al-Abed SR, Pinto PX, McKernan J et al (2017) Mechanisms and effectivity of sulfate reducing bioreactors using a chitinous substrate in treating mining influenced water. Chem Eng J 323:270–277. https://doi.org/10.1016/j.cej.2017.04.045

An C, Huang G, Yao Y, Zhao S (2017) Emerging usage of electrocoagulation technology for oil removal from wastewater: a review. Sci Total Environ 579:537–556. https://doi.org/10.1016/j.scitotenv.2016.11.062

APHA (2017) Standard Methods for the Examination of Water and Wastewater, 23rd edn. American Public Health Association, American Water Works Association, Water Environment Federation, Washington D.C

Barbosa LP, Costa PF, Bertolino SM, Silva JCC, Guerra-Sá R, Leão VA, Teixeira MC (2014) Nickel, manganese and copper removal by a mixed consortium of sulfate reducing bacteria at a high COD/sulfate ratio. World J Microbiol Biotechnol 30:2171–2180. https://doi.org/10.1007/s11274-013-1592-x

Bener S, Bulca Ö, Palas B, Tekin G, Atalay S, Ersöz G (2019) Electrocoagulation process for the treatment of real textile wastewater: Effect of operative conditions on the organic carbon removal and kinetic study. Process Saf Environ Prot 129:47–54. https://doi.org/10.1016/j.psep.2019.06.010

Box GEP, Hunter WG, Hunter JS (1978) Fractional factorial design at two levels. In: statistics for experimenters: an introduction to design, data analysis, and model building. John Wiley & Sons, Inc, New Jersey, pp 374–418

Brazil (2007) National energy plan 2030: thermoelectric generation - mineral coal. Minist. mines energy 146

Brazil (2018) 11th Report on Environmental Indicators Management - Public Civil Action nº 388 93.8000.533-4. Process nº 2000.72.04.002543-9 1–308

Brazil (2011) National Council of the Environment (CONAMA). Resolut. nº 430 1–9

Brazil (2005) National Council of the Environment (CONAMA). Resolut. nº 357 58–63

Calado V, Montgomery DC (2003) Planejamento de experimentos usando o Statistica. E-papers, Rio de Janeiro

Demers I, Benzaazoua M, Mbonimpa M, Bouda M, Bois D, Gagnon M (2015) Valorisation of acid mine drainage treatment sludge as remediation component to control acid generation from mine wastes, part 1: material characterization and laboratory kinetic testing. Miner Eng 76:109–116. https://doi.org/10.1016/j.mineng.2014.10.015

Fogler HS (1999) Elements of chemical reaction engineering, 3rd edn. Prentice Hall, 967 p. New Jersey

Follmann HVDM, Souza E, Battistelli AA et al (2020) Determination of the optimal electrocoagulation operational conditions for pollutant removal and filterability improvement during the treatment of municipal wastewater. J Water Process Eng 36:1–10. https://doi.org/10.1016/j.jwpe.2020.101295

Guimarães D, Leão VA (2014) Batch and fixed-bed assessment of sulphate removal by the weak base ion exchange resin Amberlyst A21. J Hazard Mater 280:209–215. https://doi.org/10.1016/j.jhazmat.2014.07.071

Helfferich FG (2004) Concepts, definitions, conventions, and notation. In: Comprehensive Chemical Kinetics. Elsevier, vol. 40, pp 7–16

Hossini H, Makhdoumi P, Rastegar SO et al (2015) Optimization of the electrocoagulation process for sulfate removal using response surface methodology. Bulg. Chem. Commun. 47:63–71

Kaur G, Couperthwaite SJ, Hatton-Jones BW, Millar GJ (2018) Alternative neutralisation materials for acid mine drainage treatment. J Water Process Eng 22:46–58. https://doi.org/10.1016/j.jwpe.2018.01.004

Kefeni KK, Msagati TAM, Mamba BB (2017) Acid mine drainage: prevention, treatment options, and resource recovery: a review. J Clean Prod 151:475–493. https://doi.org/10.1016/j.jclepro.2017.03.082

Kefeni KK, Msagati TM, Maree JP, Mamba BB (2015) Metals and sulphate removal from acid mine drainage in two steps via ferrite sludge and barium sulphate formation. Miner Eng 81:79–87. https://doi.org/10.1016/j.mineng.2015.07.016

Levenspiel O (1999) Chemical reaction engineering, 3rd edn. John Wiley & Sons, 684 p. New York

Macan JM, Teixeira GA, Pich CT et al (2012) Avaliação da toxicidade de drenagem ácida de mina de carvão, utilizando parâmetros físico-químicos e bioensaios. Rev. Bras. Biociências 10:275–280

Mamelkina MA, Cotillas S, Lacasa E, Sáez C, Tuunila R, Sillanpää M, Häkkinen A, Rodrigo MA (2017) Removal of sulfate from mining waters by electrocoagulation. Sep Purif Technol 182:87–93. https://doi.org/10.1016/j.seppur.2017.03.044

Mamelkina MA, Tuunila R, Sillänpää M, Häkkinen A (2019) Systematic study on sulfate removal from mining waters by electrocoagulation. Sep Purif Technol 216:43–50. https://doi.org/10.1016/j.seppur.2019.01.056

Masindi V, Osman MS, Abu-Mahfouz AM (2017) Integrated treatment of acid mine drainage using BOF slag, lime/soda ash and reverse osmosis (RO): Implication for the production of drinking water. Desalination 424:45–52. https://doi.org/10.1016/j.desal.2017.10.002

Mesa V, Gallego JLR, González-Gil R, Lauga B, Sánchez J, Méndez-García C, Peláez AI (2017) Bacterial, archaeal, and eukaryotic diversity across distinct microhabitats in an acid mine drainage. Front Microbiol 8:1–17. https://doi.org/10.3389/fmicb.2017.01756

Moodley I, Sheridan CM, Kappelmeyer U, Akcil A (2018) Environmentally sustainable acid mine drainage remediation: Research developments with a focus on waste/by-products. Miner Eng 126:207–220. https://doi.org/10.1016/j.mineng.2017.08.008

Moosa S, Nemati M, Harrison STL (2005) A kinetic study on anaerobic reduction of sulphate, part II: Incorporation of temperature effects in the kinetic model. Chem Eng Sci 60:3517–3524. https://doi.org/10.1016/j.ces.2004.11.036

Najib T, Solgi M, Farazmand A, Heydarian SM, Nasernejad B (2017) Optimization of sulfate removal by sulfate reducing bacteria using response surface methodology and heavy metal removal in a sulfidogenic UASB reactor. J Environ Chem Eng 5:3256–3265. https://doi.org/10.1016/j.jece.2017.06.016

Nariyan E, Sillanpää M, Wolkersdorfer C (2017) Electrocoagulation treatment of mine water from the deepest working European metal mine – performance, isotherm and kinetic studies. Sep Purif Technol 177:363–373. https://doi.org/10.1016/j.seppur.2016.12.042

Nariyan E, Wolkersdorfer C, Sillanpää M (2018) Sulfate removal from acid mine water from the deepest active European mine by precipitation and various electrocoagulation configurations. J Environ Manage 227:162–171. https://doi.org/10.1016/j.jenvman.2018.08.095

Nippatla N, Philip L (2019) Electrocoagulation-floatation assisted pulsed power plasma technology for the complete mineralization of potentially toxic dyes and real textile wastewater. Process Saf Environ Prot 125:143–156. https://doi.org/10.1016/j.psep.2019.03.012

Núñez-Gómez D, Alves AAA, Lapolli FR, Lobo-Recio MÁ (2017a) Application of the statistical experimental design to optimize mine-impacted water (MIW) remediation using shrimp-shell. Chemosphere 167:322–329. https://doi.org/10.1016/j.chemosphere.2016.09.094

Núñez-Gómez D, Lapolli FR, Nagel-Hassemer ME, Lobo-Recio MÁ (2018) Optimization of Fe and Mn removal from coal acid mine drainage (AMD) with waste biomaterials: statistical modeling and kinetic study. Waste and Biomass Valorization 1:1–15. https://doi.org/10.1007/s12649-018-0405-8

Núñez-Gómez D, Lapolli FR, Nagel-Hasssemer ME, Lobo-Recio MÁ (2017b) Optimization of acid mine drainage remediation with central composite rotatable design model. Energy Procedia 136:233–238. https://doi.org/10.1016/j.egypro.2017.10.248

Núñez-Gómez D, Nagel-Hassemer ME, Lapolli FR, Lobo-Recio MÁ (2016) Potencial dos resíduos do processamento de camarão para remediação de águas contaminadas com drenagem ácida mineral. Polímeros 26:1–7. https://doi.org/10.1590/0104-1428.1757

Núñez-Gómez D, Rodrigues C, Lapolli FR, Lobo-Recio MÁ (2019) Adsorption of heavy metals from coal acid mine drainage by shrimp shell waste: Isotherm and continuous-flow studies. J Environ Chem Eng 7:1–10. https://doi.org/10.1016/j.jece.2018.11.032

Peiravi M, Mote SR, Mohanty MK, Liu J (2017) Bioelectrochemical treatment of acid mine drainage (AMD) from an abandoned coal mine under aerobic condition. J Hazard Mater 333:329–338. https://doi.org/10.1016/j.jhazmat.2017.03.045

Rodrigues C, Núñez-Gómez D, Follmann HVDM et al (2020) Biostimulation of sulfate-reducing bacteria and metallic ions removal from coal mine-impacted water (MIW) using shrimp shell as treatment agent. J Hazard Mater (398):122893. https://doi.org/10.1016/j.jhazmat.2020.122893

Rodrigues C, Núñez-Gómez D, Silveira DD, Lapolli FR, Lobo-Recio MA (2019) Chitin as a substrate for the biostimulation of sulfate-reducing bacteria in the treatment of mine-impacted water (MIW). J Hazard Mater 375:330–338. https://doi.org/10.1016/j.jhazmat.2019.02.086

Sánchez-España J (2007) The behavior of iron and aluminum in acid mine drainage: speciation, mineralogy, and environmental significance. In: Letcher TM (ed) Thermodynamics, Solubility and Environmental Issues. Elsevier B.V. Chapter 7:137–150

Seo EY, Cheong YW, Yim GJ, Min KW, Geroni JN (2017) Recovery of Fe, Al and Mn in acid coal mine drainage by sequential selective precipitation with control of pH. Catena 148:11–16. https://doi.org/10.1016/j.catena.2016.07.022

Shamaei L, Khorshidi B, Perdicakis B, Sadrzadeh M (2018) Treatment of oil sands produced water using combined electrocoagulation and chemical coagulation techniques. Sci Total Environ 645:560–572. https://doi.org/10.1016/j.scitotenv.2018.06.387

Silva AM, Lima RMF, Leão VA (2012) Mine water treatment with limestone for sulfate removal. J Hazard Mater 221–222:45–55. https://doi.org/10.1016/j.jhazmat.2012.03.066

Silva LFO, de Vallejuelo SF-O, Martinez-Arkarazo I et al (2013) Study of environmental pollution and mineralogical characterization of sediment rivers from Brazilian coal mining acid drainage. Sci Total Environ 447:169–178. https://doi.org/10.1016/j.scitotenv.2012.12.013

Singh TSA, Ramesh ST (2014) An experimental study of CI Reactive Blue 25 removal from aqueous solution by electrocoagulation using Aluminum sacrificial electrode: Kinetics and influence of parameters on electrocoagulation performance. Desalin Water Treat 52:2634–2642. https://doi.org/10.1080/19443994.2013.794714

Tait S, Clarke WP, Keller J, Batstone DJ (2009) Removal of sulfate from high-strength wastewater by crystallisation. Water Res 43:762–772. https://doi.org/10.1016/j.watres.2008.11.008

Tolonen E-T, Hu T, Rämö J, Lassi U (2016) The removal of sulphate from mine water by precipitation as ettringite and the utilisation of the precipitate as a sorbent for arsenate removal. J Environ Manage 181:856–862. https://doi.org/10.1016/j.jenvman.2016.06.053

Vepsäläinen M (2012) Electrocoagulation in the treatment of industrial waters and wastewaters. VTT publications.154 p. Thesis (Doctor of Science), Lappeenranta University of Technology, Finland.

Vepsäläinen M, Kivisaari H, Pulliainen M, Oikari A, Sillanpää M (2011) Removal of toxic pollutants from pulp mill effluents by electrocoagulation. Sep Purif Technol 81:141–150. https://doi.org/10.1016/j.seppur.2011.07.017

Vepsäläinen M, Pulliainen M, Sillanpää M (2012) Effect of electrochemical cell structure on natural organic matter (NOM) removal from surface water through electrocoagulation (EC). Sep Purif Technol 99:20–27. https://doi.org/10.1016/j.seppur.2012.08.011

Vepsäläinen M, Sillanpää M (2020) Electrocoagulation in the treatment of industrial waters and wastewaters. In: Sillanpää M (ed) Advanced Water Treatment - Electrochemical methods. Elsevier Inc., Miami, pp 1–78

Wu M, Hu Y, Liu R, Lin S, Sun W, Lu H (2019) Electrocoagulation method for treatment and reuse of sulphide mineral processing wastewater: characterization and kinetics. Sci Total Environ 696: 134063. https://doi.org/10.1016/j.scitotenv.2019.134063